Infrared and Low-Temperature Micro-Raman Spectra of the OH Stretching Vibrations in Cummingtonite

A. WANG, P. DHAMELINCOURT, and G. TURRELL*

Laboratory of Physical Mineralogy, Academy of Geological Sciences of China, Beijing, China (A.W.); and Laboratoire de Spectrochimie Infrarouge et Raman, CNRS, Université des Sciences et Techniques de Lille Flandres Artois, Bât. C5, 59655 Villeneuve D'Ascq Cedex, France (P.D., G.T.)

A simple structural model is developed of the effect of cation occupancy on the OH stretching bands of Cummingtonite. The observed broadening of the unresolved Raman bands at low temperatures, as well as the variation in the inter- and intra-ionic force constants of the OH group, is consistent with the model. These results confirm earlier assignments of the vibrational spectra of amphiboles in the OH stretching region.

Index Headings: **Infrared; Amphiboles; Cation distribution.**

INTRODUCTION

As pointed out in the previous paper,[1] the cation distribution in amphiboles is a subject that has been of interest to mineralogists for many years. Several spectroscopic methods, such as Mössbauer and electron absorption, as well as infrared and Raman, have proved to be useful in the determination of the site occupancies in many kinds of amphiboles. These methods are complementary, although vibrational spectroscopy yields the most direct information concerning $M(1)$ and $M(3)$ site occupancy. However, it has been shown that under normal conditions neither the Raman nor the infrared instruments which are presently available can distinguish between the OH stretching bands predicted from structural considerations, for example, the components B', B'' and C', C'' of binary systems which were defined previously.[1] Thus only the total occupancy of the $M(1)$ and $M(3)$ sites by each cation could be determined from the experimental data. Any estimate of individual $M(1)$ or $M(3)$ site occupancy involved approximations which in certain cases led to inaccuracies.

In the present work a variable-temperature microscope stage was used to maintain the microcrystalline samples at constant low temperatures in the range +20°C to −190°C during the Raman measurements. The objective of this experiment was to reduce the linewidths of the OH bands in an attempt to resolve the predicted fine structure.

Another question arose in the spectroscopic investigation of cation site occupancy in amphiboles. Namely, it is assumed that the relative intensities of the OH stretching bands in the vibrational spectra provide direct measures of the occupancy of the $M(1)$ and $M(3)$ sites by the various cations.[2] However, the assignments in the band patterns observed in the 3600–3700 cm^{-1} region have never been verified; for example, the effect of cation characteristics such as atomic mass, ionic radius, and electronegativity on the OH stretching frequencies have not been established. In this work, the intra- and inter-ionic force constants of the OH groups in the crystal are determined. Because mineralogical samples are generally mixtures of crystals having slightly different compositions, precise measurements of the micro-Raman and micro-infrared spectra were performed on the same single particle of a Cummingtonite sample.

A model is proposed in order to establish a relationship between the characteristics of the site-occupant cations and the force constants determined from the analysis of the OH spectral patterns. Finally, by the use of this model it is demonstrated that the usual assignments are quite reasonable. Furthermore, the same model provides an explanation for the observed unusual low-temperature behaviors of the OH stretching bands.

THEORETICAL ANALYSIS

The space group of Cummingtonite is $C2/m = C_{2h}^3$, with unit-cell parameters a = 9.51 Å, b = 18.19 Å, c = 5.33 Å, and $\beta = 101°55'$.[3] As the lattice is monoclinic side-centered, the volume of the unit cell is twice the volume of the primitive cell used in the analysis of vibrational spectra.[4] The composition of the primitive cell can be represented by the formula $M_7Si_8O_{22}(OH)_2$. Thus there are 120 degrees of vibrational freedom for the optical modes and the reduced representation has the structure

$$\Gamma_{vib} = 30\,A_g + 30\,B_g + 27\,A_u + 33\,B_u. \qquad (1)$$

These modes can be classified with the help of the correlation method (see Ref. 5 and table II of Ref. 1). The 60 *gerade*-species modes are Raman-active. In principle, the A_g and B_g species vibrations can be distinguished by Raman polarization measurements using the backscattering $Z(XX)\bar{Z}$ and $Z(XY)\bar{Z}$ configurations, as the polarizability tensors have the forms

$$\begin{pmatrix} a & & d \\ & b & \\ d & & c \end{pmatrix}$$

for the A_g modes and

$$\begin{pmatrix} & e & \\ e & & f \\ & f & \end{pmatrix}$$

for the B_u modes. The 60 *ungerade*-species vibrations are infrared-active; in principle they can be distinguished with the help of polarized light, as the dipole-moment variations for the A_u-species vibrations are along the z-axis of the crystal. This method has been applied in a study

Received 15 January 1988.
* Author to whom correspondence should be sent.

0003-7028/88/4208-1451$2.00/0

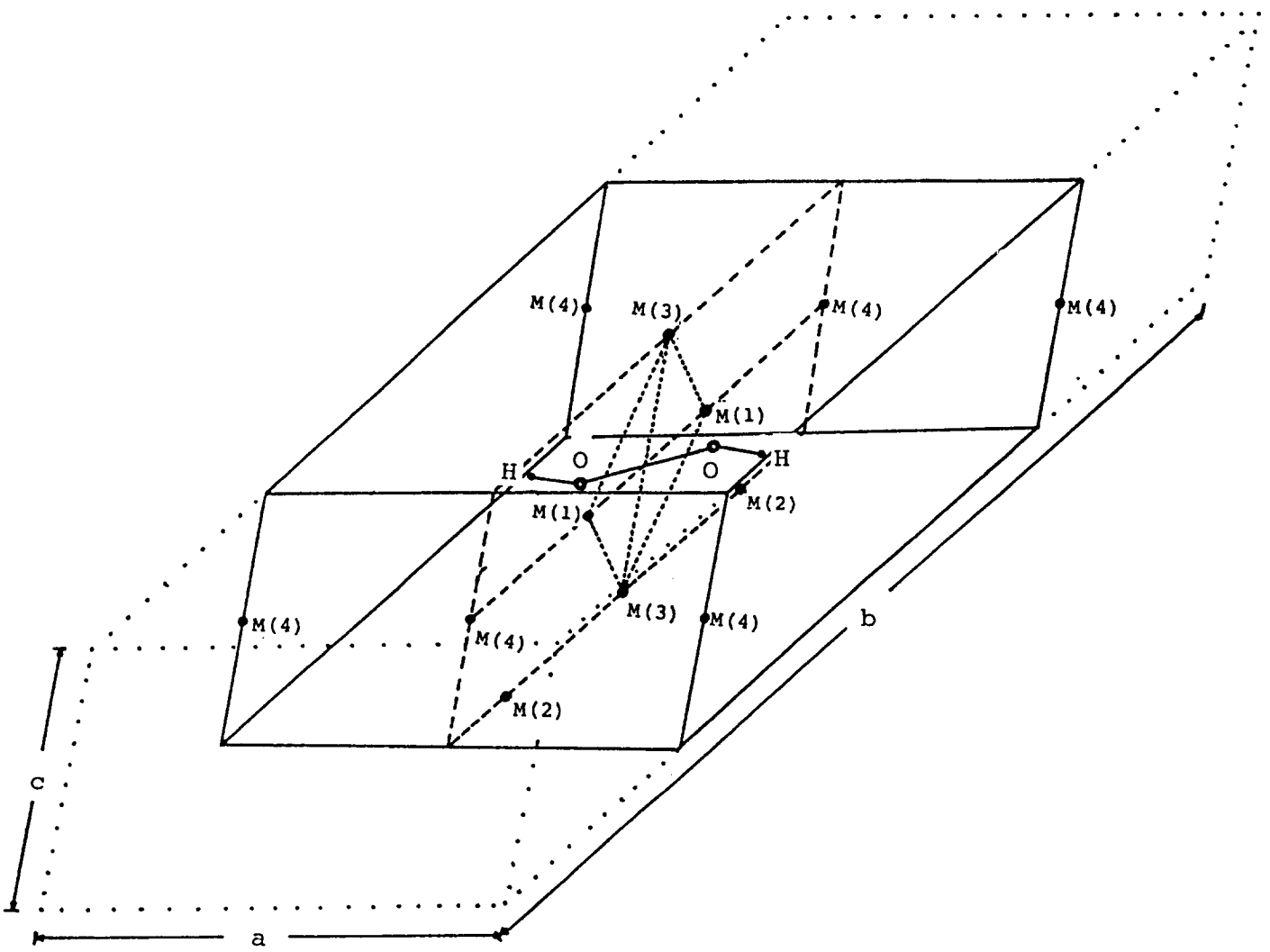

FIG. 1. $(OH)^-$ groups in the primitive cell of Cummingtonite structure.

of mica.[6] However, it should be noted that the preparation of suitably oriented micro-samples is often very difficult.

The primitive cell of Cummingtonite contains two OH groups which point toward a central void (Fig. 1). This structure is in good agreement with the recorded infrared spectrum, which clearly shows that there is no hydrogen bonding.[2] In Cummingtonite the M in the general formula represents Mg^{2+} and Fe^{2+}, which occupy $M(1)$, $M(2)$, $M(3)$, and $M(4)$ sites. As discussed in the previous article,[1] the $M(3)$ and the two $M(1)$ sites form a nearly equilateral triangle around each OH group (Fig. 1). The change in their occupants (Mg^{2+} or Fe^{2+}) with different ionic radius and electronegativity will modify the force field and, therefore, the frequency pattern of the OH stretching modes.

Cummingtonite can be considered to be a binary system. Thus, there are four configurations, and six OH bands (A, B', B'', C', C'', and D) should be observable in the 3600–3700 cm^{-1} region. However, the spectral patterns usually consist of four bands because the bands designated B' and B'', and C' and C'', overlap to give only two bands—B and C, respectively. Furthermore, as there are two OH groups in the primitive unit cell, Davydov coupling is permitted. Factor-group analysis (see table IV of Ref. 1) leads to the prediction of two fundamental stretching modes, *viz.*,

$$\Gamma_{vib} = A_g(\mathrm{R}) + B_u(\mathrm{IR}). \tag{2}$$

The modes A_g and B_u correspond, respectively, to the in-phase and out-of-phase stretching vibrations of the two OH groups. Therefore, in the Raman and infrared spectra of Cummingtonite, four analogous spectral patterns (A, B, C, D) are expected to be observed, corresponding to different vibrational species.

The vibrational frequencies of the OH groups can be related to appropriate force constants with the use of the GF matrix method.[4] As the two OH groups have no atom in common, coupling results only from the interaction potential; thus, in terms of the symmetry coordinates

$$\mathbf{S} = \begin{pmatrix} \frac{1}{\sqrt{2}}(\Delta r_1 + \Delta r_2) \\ \frac{1}{\sqrt{2}}(\Delta r_1 - \Delta r_2) \end{pmatrix}; \tag{3}$$

the potential energy is given by

$$2V = \tilde{\mathbf{S}}\mathbf{F}\mathbf{S} \tag{4}$$

where $\tilde{\mathbf{S}}$ is the transpose of $\mathbf{S}$ and

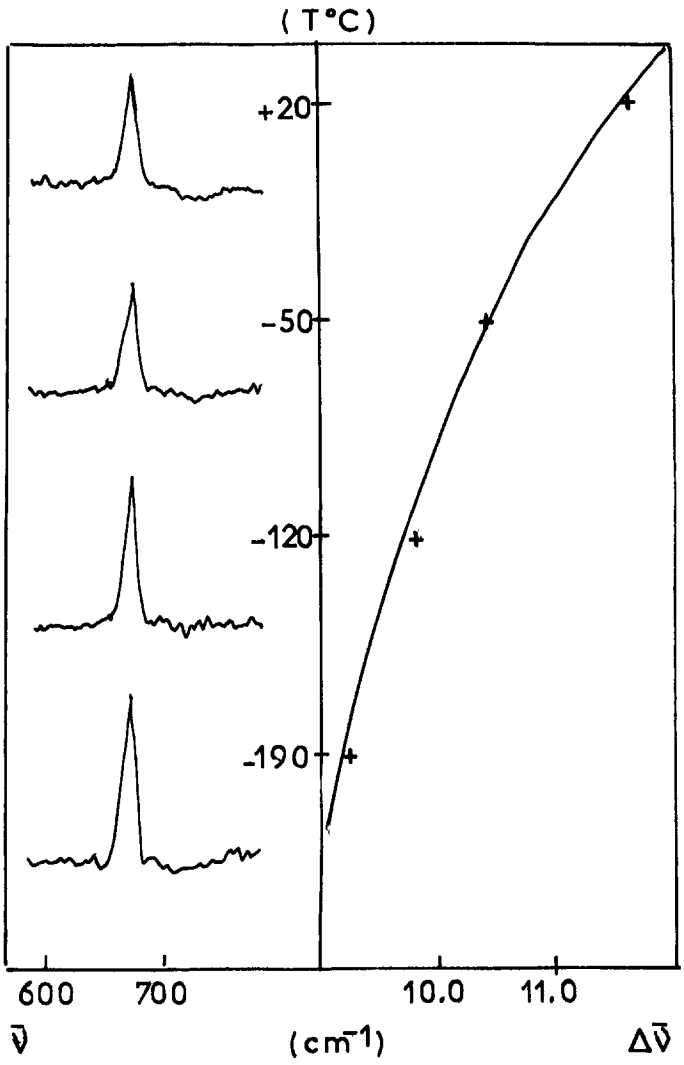

FIG. 2. The 670-cm^{-1} band and its bandwidth as a function of temperature.

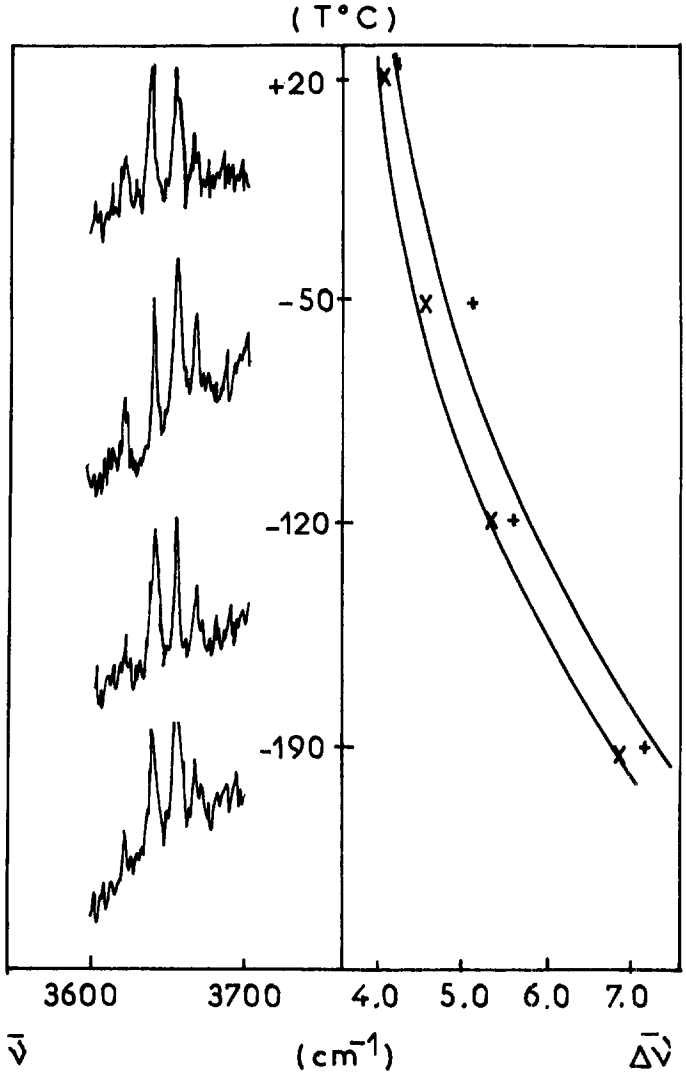

FIG. 3. The OH stretching bands and their bandwidth as a function of temperature.

$$\mathbf{F} = \begin{pmatrix} f + f' & 0 \\ 0 & f - f' \end{pmatrix} \tag{5}$$

with f and f' the intra- and inter-OH force constants, respectively. The kinetic energy of the OH vibrations is given by

$$2\mathbf{T} = \dot{\mathbf{S}}\mathbf{G}^{-1}\dot{\mathbf{S}}, \tag{6}$$

where **G** in terms of symmetry coordinates becomes

$$\mathbf{G} = \begin{pmatrix} \mu_O + \mu_H & 0 \\ 0 & \mu_O + \mu_H \end{pmatrix} \tag{7}$$

and μ_O and μ_H are the reciprocal masses of the oxygen and hydrogen atoms, respectively. The secular determinant, which then takes the form

$$| GF - E\lambda_k | = 0, \qquad k = 1, 2 \tag{8}$$

leads directly to the relations

$$\lambda_1 = 4\pi^2 c^2 \tilde{\nu}_1^2 = (\mu_H + \mu_O)(f + f') \tag{9a}$$

for the A_g mode and

$$\lambda_2 = 4\pi^2 c^2 \tilde{\nu}_2^2 = (\mu_H + \mu_O)(f - f') \tag{9b}$$

for the B_u mode, from which the force constants can be calculated from the observed infrared and Raman frequencies.

EXPERIMENTS AND RESULTS

Low-temperature Experiments. The variable-temperature stage used in this work was a TH600 heating-freezing stage developed by Linkan Scientific Instruments (U.K.). The working temperature range was −196°C to +600°C, with 0.1°C as the reading accuracy and ±1°C as the controlled stability. The stage was mounted in the microscope of a micro-Raman spectrometer, MOLE

TABLE I. Results of the Raman and infrared experiments and the force constant calculation.

Configuration	Frequency of vibrational band			Force constant	
	ν_{A_g} (cm^{-1})	ν_{B_u} (cm^{-1})	$\Delta\nu = \nu_{A_g} - \nu_{B_u}$ (cm^{-1})	f (m dyn/Å)	f'(m dyn/Å)
A	3665.92	3666.91	−0.99	7.5189	−0.0020
B	3652.56	3653.14	−0.58	7.4634	−0.0012
C	3636.14	3637.74	−1.60	7.3985	−0.0033
D	3617.19	3618.61	−1.42	7.3212	−0.0029

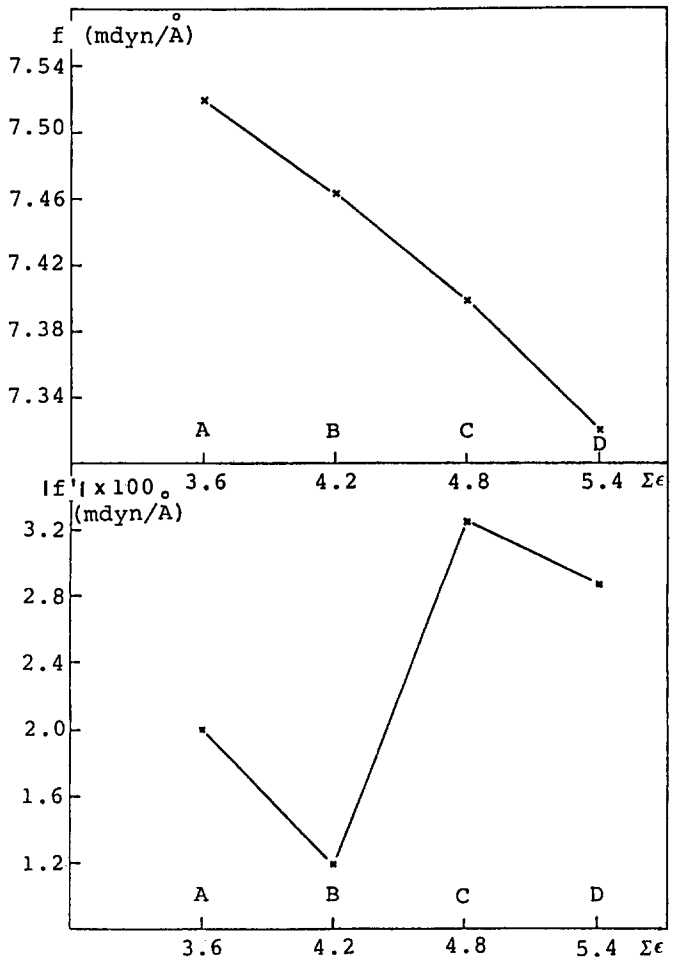

FIG. 4. The force constants of the OH groups as a function of the $M(1)$ and $M(3)$ cation site configuration.

(Jobin-Yvon, France). A reservoir of liquid nitrogen fed the freezing stage by means of a temperature-controlled inlet.

The experiments were performed from room temperature down to that of liquid nitrogen. For each temperature the system was allowed to reach equilibrium before the Raman spectra were measured. The OH stretching region (3600–3700 cm^{-1}) was recorded at a number of temperatures from 20°C to −190°C. Spectra in the region 1200 to 100 cm^{-1} were also recorded under the same conditions. The results presented in Fig. 2 show that in the latter region the fundamental band at ~670 cm^{-1} (species A_g) exhibits its usual behavior at low temperature, e.g., its linewidth decreases with decreasing temperature. On the other hand, the spectra in the OH stretching region show that the linewidths of the bands B and C increase significantly when the sample temperature decreases to that of liquid nitrogen (Fig. 3). The temperature dependence of the A and D bands was difficult to determine, as their intensities were only slightly above the noise level.

Observed Spectra and Force Constants. As pointed out above, the stretching and interaction force constants of the OH groups can be calculated from the frequencies measured in the Raman and infrared spectra. To obtain results which are internally consistent, one must perform the Raman and infrared measurements on the same particle, and the frequencies must be measured as accurately as possible. Therefore, in this work several well-formed microcrystals of Cummingtonite were chosen, and their infrared spectra were recorded. An infrared microscope mounted on a Bruker IFS-45 spectrometer was employed. The wavenumber accuracy was better than 0.1 cm^{-1}. The Raman spectra were measured on an OMARS 89 multichannel Raman instrument equipped with a microscope produced by DILOR (France). As the standard lines of a neon lamp were recorded at the same time for calibration, the wavenumbers of the Raman bands could be obtained with the same accuracy. The decomposition of the spectral features was then performed in order to obtain precise wavenumber values for each OH band. These results were then used to calculate the force constants (Table I). The values of the principal constant f obtained in this work are in good agreement with the results given in the literature for the OH bond. The value of the interaction force constant f' is about 400 times less than that of f, a result which would appear to be reasonable for the coupling between the two OH groups.

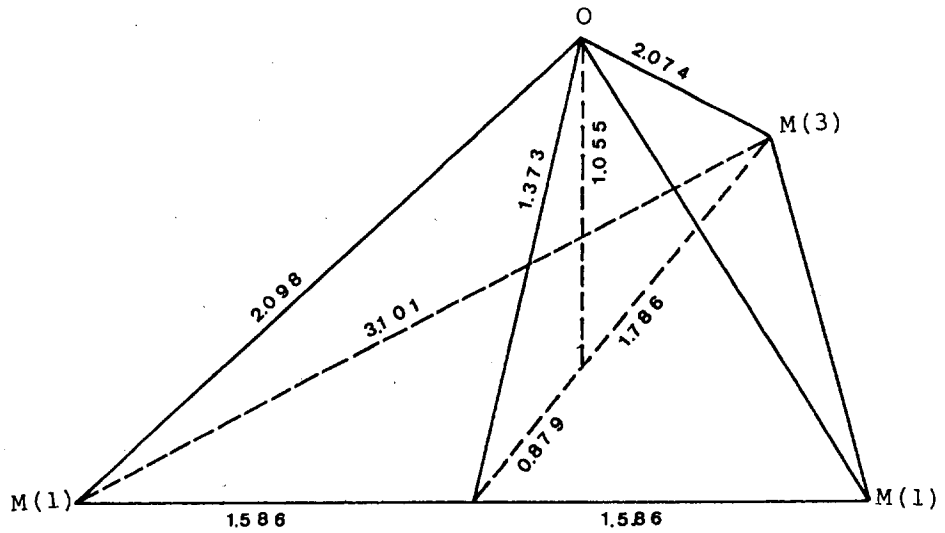

FIG. 5. Local structure in the unit cell of Cummingtonite.

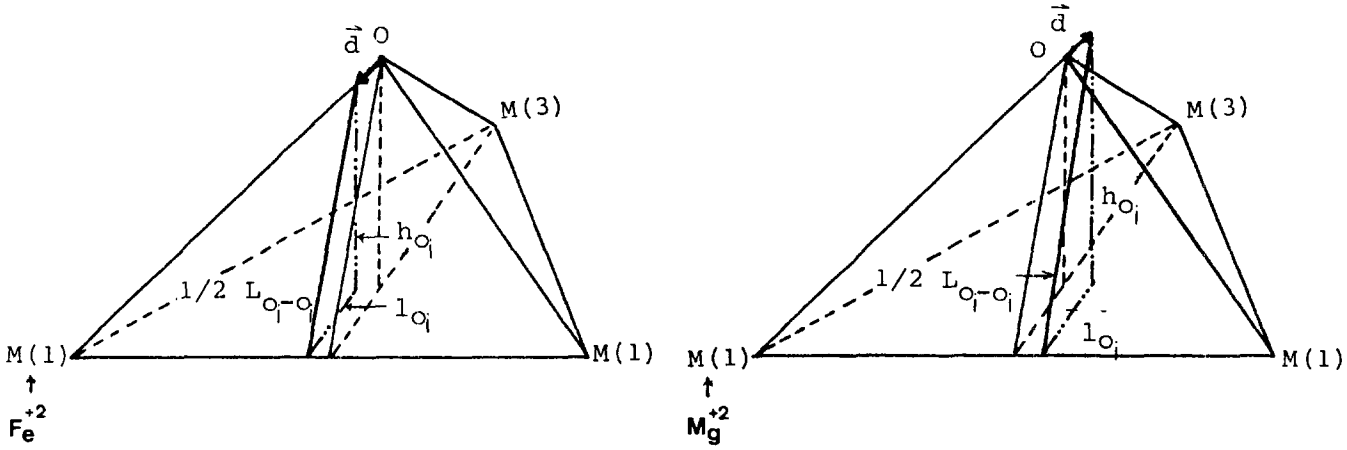

FIG. 6. The calculated distances in the model.

DISCUSSION

As shown in Fig. 4, the force constant f decreases monotonically in the order of the configuration A, B, C, and D, while the change in f' is more complex. In order to explain this phenomenon and establish a relation between the spectral data and the characteristics of the occupant cations in the $M(1)$ and $M(3)$ sites, we propose the following model: The OH group is considered to be an isolated diatomic ion. Its stretching frequency is proportional to $(f/\mu)^{1/2}$, where μ is the reduced mass. The force constant f depends on the distance between the oxygen and hydrogen atoms (L_{OH}), which is a function of the cation environment. Thus, from the change in the OH bond length due to the variation of the occupancy situation in the $M(1)$ and $M(3)$ sites, the relationship of f to the properties of the occupant cations can be determined. On the other hand, as each OH group is dipolar, the interaction between the two dipoles in the unit cell is represented by the potential energy $-p_1 \cdot p_2/R^3$, where p_i is the dipole moment of ion i. Thus, the relation between the values of f' and the properties of the occupant cations can also be established as a function of the distance R ($L_{OH\text{-}OH}$)between the two OH groups.

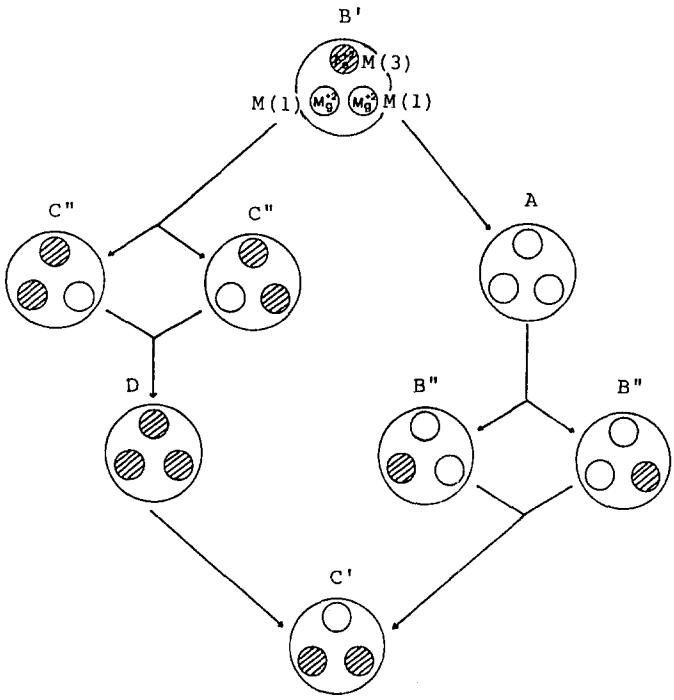

FIG. 7. Calculation procedure for the different cation configurations on $M(1)$ and $M(3)$ sites.

Figure 5 shows the local structure of Cummingtonite in which the distances between the atoms have been calculated on the basis of the results of crystal-structure refinement.[3] In this case, with the substitution of a Mg^{2+} ion by a Fe^{2+} ion in any $M(j)$ site, two effects which could induce a change in the OH distance ($L_{O\text{-}H}$), as well as that between the two OH groups ($L_{OH\text{-}OH}$), must be considered. First, the displacement of the oxygen and hydrogen atoms ("pushing effect") due to the entrance of larger cations into the structure must be considered. This effect will increase the distance $L_{OH\text{-}OH}$ and perhaps $L_{O\text{-}H}$. The second effect is due to a change in the electronegativity of the occupant ion. When the electronegativity increases, the interaction between the cation in the $M(j)$ site and the oxygen atom becomes more covalent. As a result, the distance between the oxygen and the cation decreases, while the distance between the hydrogen atom and the cation increases. Therefore, the two distances $L_{O\text{-}H}$ and $L_{OH\text{-}OH}$ are modified. Of these two effects only the second one has a significant influence on $L_{O\text{-}H}$. It should be noted from the experimental results that it is the principal force constant f, which is directly related to the distance $L_{O\text{-}H}$, that exhibits a large variation. Therefore, in a first approximation, only the effect of the electronegativity of the cation will be considered.

In order to simplify the model, we calculate only the displacement of oxygen atoms. The vertical distance between the oxygen atom and the line connecting the $M(1)$ and $M(1)'$ sites in certain configurations $i(i = A, B \ldots)$ is represented by $L_{O_i\text{-}O_i}/2$. The vertical distance h_{O_i} between an oxygen and the $M(1)$, $M(3)$, $M(1)'$ plane has an inverse behavior with respect to that of $L_{O\text{-}H}$, e.g., when h_{O_i} decreases, h_{H_i} [the distance between a hydrogen and the $M(1)$, $M(3)$, $M(1)'$ plane] increases and the $L_{O_i\text{-}H_i}$ distance increases. A parameter d has been chosen which represents the value of the displacement of the oxygen atom in the direction of $O_iM(j)$, depending on the substitution, as shown in Fig. 6. In the calculation, the value of d has been stepped from 0.01 Å to 0.5 Å.

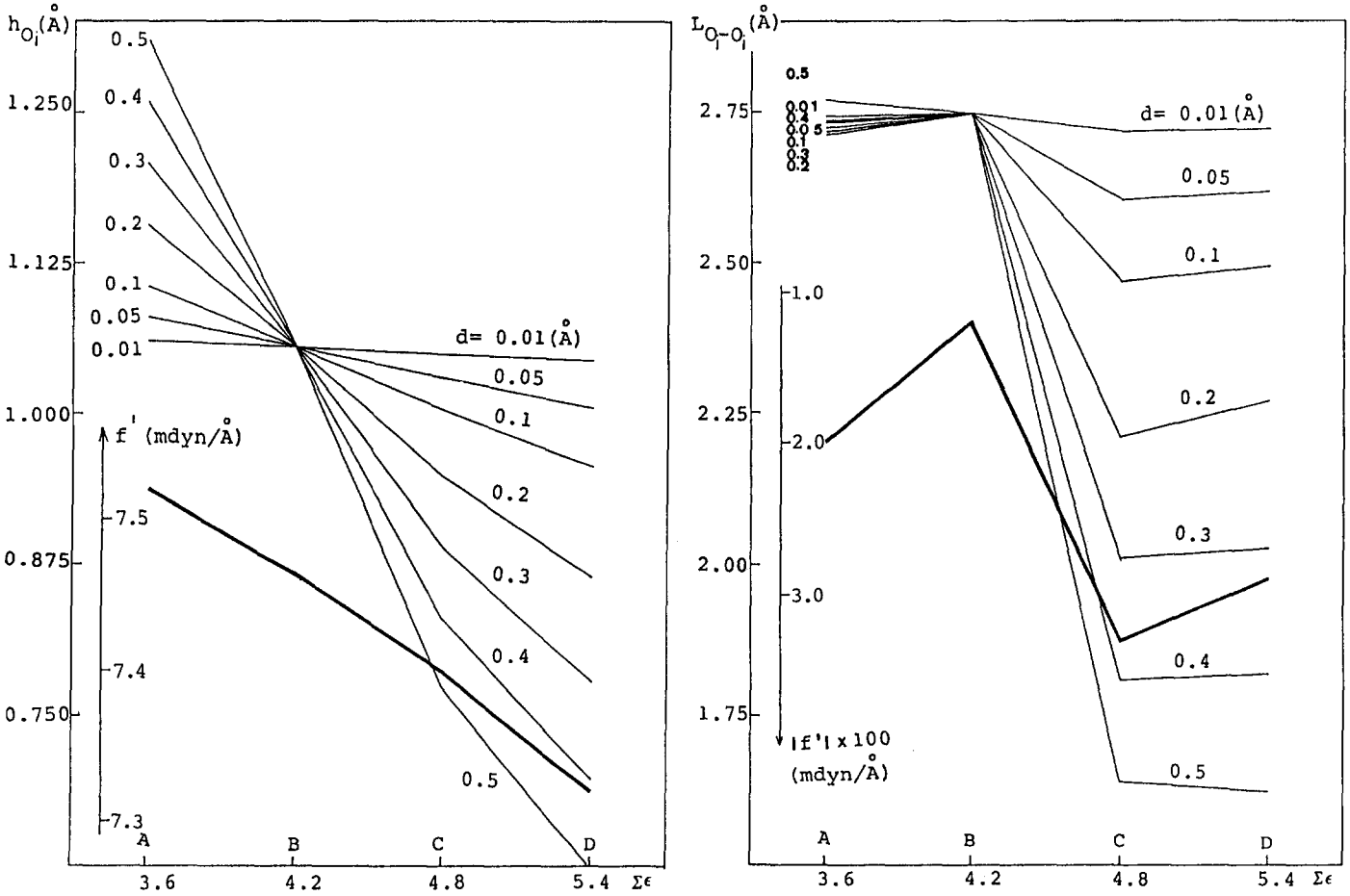

FIG. 8. The calculated distances as a function of total electronegativity of the cation configurations, where d is the displacement parameter.

In Ghose's work,[3] which is the basis of the following calculation, the sample was assumed to have the composition $(Mg_{4.05}Fe_{2.50}Mn_{0.17}Ca_{0.35})(Si_{7.9}Al_{0.1}O_{22})(OH)_2$. Thus, the configuration with the highest probability is $Mg_2^{2+}Fe^{2+}$, and the simplest arrangement, B' – 2 Mg^{2+}-$M(1)Fe^{2+}M(3)$, which ensures that the proper crystal symmetry (C_{2h}^3), was chosen initially. Figure 7 shows that there are two ways to change the occupancy situation B' if only one cation is changed at a time. The distances h_{O_i}, l_{O_i}, and ½ $L_{O_i\text{-}O_i}$ for each occupancy situation can then be calculated from the formula given in Table II. The results of the calculation are shown in Fig. 8 as a function of the parameter d. They show that the distances h_{O_i} change in the same direction as that of the

TABLE II. Formula for the model calculation.

$$\tfrac{1}{2}L_{O_i-O_i} = (h_{O_i}^2 + l_{O_i}^2)^{1/2}$$

B'	A	B''	C'
$h_{O_{B'}} = 1.055$	$h_{O_A} = h_{O_{B'}} + d \sin\theta$	$h_{O_{B''}} = h_{O_A} - d \sin\alpha$	$h_{O_{C'}} = h_{O_{B''}} - d \sin\beta$
$l_{O_{B'}} = 0.879$	$l_{O_A} = l_{O_{B'}} - d \cos\theta$	$l_{O_{B''}} = l_{O_A} - d \cos\alpha \sin\alpha$	$l_{O_{C'}} = l_{O_{B''}} - d \cos\beta \sin\beta$
	$tg\theta = \dfrac{1.055}{1.786}$	$tg\alpha = \dfrac{h_{O_A}}{(l_{O_A}^2 + 1.586^2)^{1/2}}$	$tg\beta = \dfrac{h_{O_{B''}}}{(l_{O_{B''}} + (1.586 + d \cos\alpha \cos\alpha)^2)^{1/2}}$
		$tg\alpha = \dfrac{l_{O_A}}{1.586}$	$tg\beta = \dfrac{l_{O_{B''}}}{1.586 + d \cos\alpha \cos\alpha}$

B'	C''	D	C'
$h_{O_{B'}} = 1.055$	$h_{O_{C''}} = h_{O_{B'}} - d \sin\gamma$	$h_{O_D} = h_{O_{C''}} - d \sin\phi$	$h_{O_{C'}} = h_{O_D} + d \sin\psi$
$l_{O_{B'}} = 0.879$	$l_{O_{C''}} = l_{O_{B'}} - d \cos\gamma \sin\gamma$	$l_{O_D} = l_{O_{C''}} - d \cos\phi \sin\phi$	$l_{O_{C'}} = l_{O_D} - d \cos\psi \sin\psi$
	$tg\gamma = \dfrac{1.055}{(0.879^2 + 1.586^2)^{1/2}}$	$tg\phi = \dfrac{l_{O_{C''}}}{(l_{O_{C''}}^2 + (1.586 + d \cos\gamma \cos\gamma)^2)^{1/2}}$	$tg\psi = \dfrac{h_{O_D}}{((2.665 - l_{O_D})^2 + d^2(\cos\phi \cos\phi - \cos\gamma \cos\gamma)^2)^{1/2}}$
	$tg\gamma = \dfrac{0.879}{1.586}$	$tg\phi = \dfrac{l_{O_{C''}}}{1.586 + d \cos\gamma \cos\gamma}$	$tg\psi = \dfrac{d(\cos\phi \cos\phi - \cos\gamma \cos\gamma)}{2.665 - l_{O_D}}$

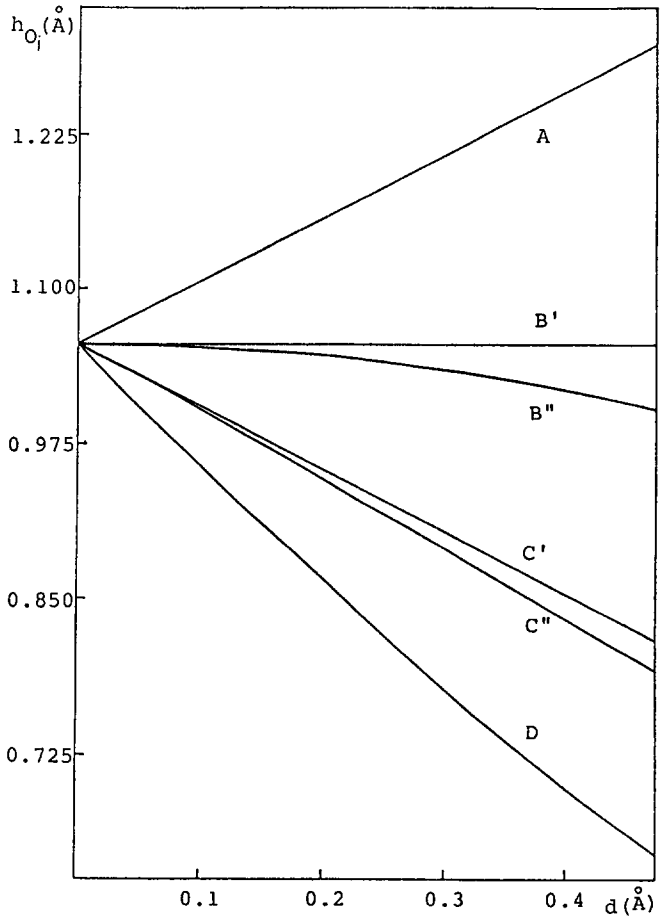

FIG. 9. The calculated distance h_{O_i} as a function of the parameter d (simulating the change of temperature).

OH stretching force constant f, while the $L_{O_i\text{-}O_i}$ distances change in the opposite direction to the coupling constant f'. This calculation then supports the previous assignments, *viz.*, different OH bands arise from the different occupancy of cations in $M(1)$ and $M(3)$ sites. It also confirms the conclusion that the observed changes in the force constants are mainly due to the different cation electronegativities.

On the order hand, Fig. 9 shows that the separations between the B' and B'' bands and the C' and C'' bands still increase with an increase in the value of the parameter d. For small values of d, the bands almost completely overlap; but when the temperature of the samples decreases, the crystal field becomes stronger. This effect can be simulated by increasing the value of d. Thus, the increasing linewidths of the OH bands at lower temperatures can be directly related to the increasing distances between the components B', B'' and C', C'', even though their bandwidths are decreasing. Nevertheless, the distance between the components remains much smaller than the spectral resolution of the instrument. Even at the lowest temperatures obtainable, the predicted doublets cannot be resolved, and the greater separation between the components appears as an apparent increase in the linewidths, in agreement with the experimental observations.

CONCLUSIONS

In the work reported in this communication an attempt has been made to resolve the overlapping components of the B and C bands of Cummingtonite with the application of low-temperature techniques. Earlier assignments of the spectral features have been confirmed with the aid of force-constant calculations. The results have been interpreted on the basis of a simple model, which also accounts for the temperature dependence of the observed bandwidths.

ACKNOWLEDGMENT

We should like to thank B. De Bettignies for providing us with the band-decomposition program used in this work.

1. A. Wang, P. Dhamelincourt, and G. Turrell, Appl. Spectrosc. **42**, 1441 (1988).
2. R. G. Burns and R. G. J. Strens, Science **153**, 890 (1966).
3. S. Ghose, Acta Cryst. **14**, 622 (1961).
4. G. Turrell, *Infrared and Raman Spectra of Crystals* (Academic Press, London, 1972).
5. W. G. Fateley, F. R. Dollish, N. T. McDevitt, and F. F. Bentley, *Infrared and Raman Selection Rules for Molecular and Lattice Vibrations: The Correlation Method* (Wiley-Interscience, New York, 1972).
6. W. Vedder, Amer. Mineral. **49**, 736 (1964).